Carrier Recovery Enhancement for Maximum-Likelihood Doppler Shift Estimation in Mars Exploration Missions

Federico S. Cattivelli, *Student Member, IEEE*, Polly Estabrook, Edgar H. Satorius, *Member, IEEE*, and Ali H. Sayed, *Fellow, IEEE*

***Abstract*—One of the most crucial stages of the Mars Exploration Missions is the Entry, Descent, and Landing (EDL) phase. During EDL, maintaining reliable communication from the spacecraft to Earth is extremely important for the success of future missions, especially in case of mission failure. EDL is characterized by very deep accelerations, caused by friction, parachute deployment and rocket firing among others. These dynamics cause a severe Doppler shift on the carrier communications link to Earth. Methods have been proposed to estimate the Doppler shift based on Maximum Likelihood. So far these methods have proved successful, but it is expected that the next Mars mission, known as the Mars Science Laboratory, will suffer from higher dynamics and lower SNR. Thus, improving the existing estimation methods becomes a necessity. We propose a Maximum Likelihood approach that takes into account the power in the data tones to enhance carrier recovery, and improve the estimation performance by up to 3 dB. Simulations are performed using real data obtained during the EDL stage of the Mars Exploration Rover B (MERB) mission.**

***Index Terms*—Doppler effect, frequency estimation, maximum-likelihood estimation, space vehicle communication.**

I. Introduction

NASA'S Viking missions made history when they became the first spacecraft to land safely on Mars in 1976. The next landing was accomplished twenty years later by the 1996 Pathfinder mission, which introduced innovative landing techniques. The two Mars Exploration Rover (MER) missions named MERA and MERB were launched by NASA in mid 2003, landing the rovers on Mars on January 2004. These rovers have travelled for miles across the Martian surface, conducting field geology and making atmospheric observations.

NASA's next mission requiring safe landing on the surface of Mars is known as the Mars Science Laboratory (MSL), and is planned for the Mars launch opportunity in 2009. The primary objective is to investigate the habitability of Mars (i.e., its capacity to sustain life) [1]. One of the most outstanding characteristics of MSL compared to previous Mars Exploration missions is the advanced landing techniques that will be employed. The Mars Entry, Descent, and Landing (EDL) stages of the MSL mission will deliver a larger rover to a higher altitude, while maintaining precision landing [2], providing access to previously unaccessible sites [2]–[4].

Manuscript received November 01, 2007; revised July 21, 2008. Current version published December 10, 2008. This work was supported by a Grant from the Jet Propulsion Laboratory under award 1276256 and by National Science Foundation (NSF) awards ECS-0601266 and ECS-0725441. The associate editor coordinating the review of this manuscript and approving it for publication was Prof. Alle-Jan van der Veen.

F. S. Cattivelli and A. H. Sayed are with the Department of Electrical Engineering, University of California, Los Angeles, CA 90095 USA (e-mail: fcattiv@ee.ucla.edu; sayed@ee.ucla.edu).

P. Estabrook and E. H. Satorius are with the Jet Propulsion Laboratory, Pasadena, CA 91109 USA (e-mail: Polly.Estabrook@jpl.nasa.gov; satorius@jpl.nasa.gov).

Digital Object Identifier 10.1109/JSTSP.2008.2005289

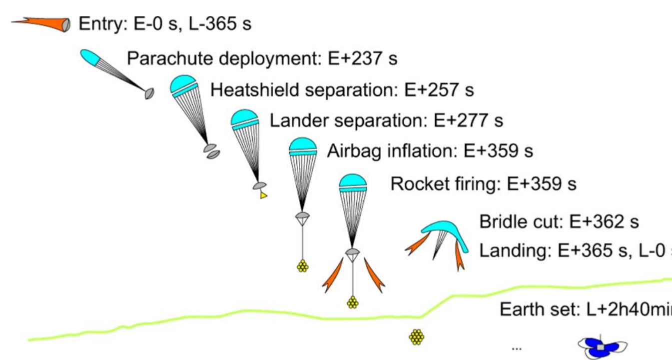

Fig. 1. Entry, Descent, and Landing stages during MER missions (from [5]).

A. Entry, Descent and Landing

The EDL stages of the mission refer to those stages between the point when the shuttle enters the atmosphere of Mars and when it finally lands on its surface. Fig. 1 shows the EDL stages for the 2004 Mars Exploration Missions [6], [5].

During EDL, it is highly important to maintain communication between the spacecraft and Earth, since the information sent could be critical for the success of future missions, especially in the eventuality of a mission failure. Before Entry and until the lander is separated from the backshell, communication is by a direct-to-Earth (DTE) X-band (8.4 GHz) link. After separation the backshell antenna can no longer be used, and communication is achieved using two links: a main UHF relay link to the Mars Odyssey or Mars Global Surveyor spacecraft, and a backup DTE link using the rover antenna. The DTE link uses a special form of MFSK modulation that transmits one out of 256 possible data tones every 10 s. This form of modulation will be discussed in the next section.

EDL is the most challenging phase of the spacecraft to ground communications [6]. There exist several phenomena that continuously accelerate and decelerate the spaceship during EDL, such as atmospheric friction and parachute deployment during Entry, bridle descent, swinging on bridle, rocket firing and bridle

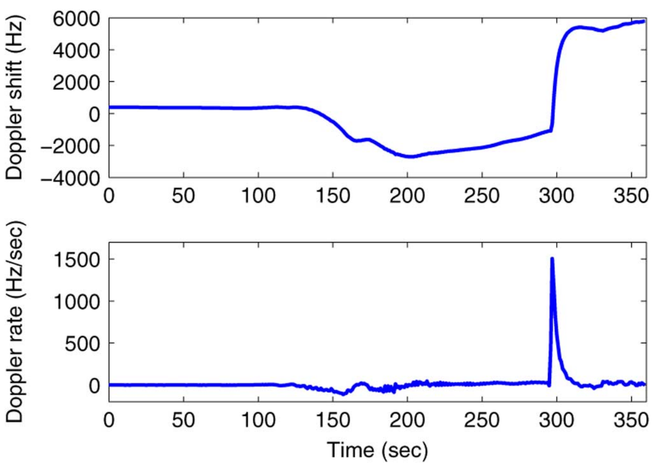

Fig. 2. Frequency profile of MERA during EDL.

separation during Descent, and bouncing on the Landing stage. All these factors contribute to the effect known as Doppler shift, where the frequency of the main carrier of the communications signal is shifted from its nominal value. Fig. 2 shows the residual frequency profile observed during the EDL stage of the MERB mission. It can clearly be observed that the Doppler shift ranges between -3 and 6 kHz. This range refers to the frequency residual which results after a first stage of Doppler shift correction; the actual Doppler shift has a range of about 90 kHz (see [5] for example). The Doppler rate, defined as the derivative of the Doppler shift, ranges between -200 and 200 Hz/s, except during parachute deployment where it can reach 1000 Hz/s.

For the 2009 Mars Science Laboratory mission, both higher Doppler shifts and Doppler rates are expected This is due to the landing techniques of the new mission, which requires landing a load of about 1000 kg, nearly twice as that of the MER missions and with a tighter landing ellipse. Predicted Doppler shifts for the MSL mission range within 15 kHz, and predicted Doppler rates are in the range -600 to 300 Hz/s. Also, since the shuttle will be able to land in areas farther away, a lower SNR is expected (possibly 0.5 to 3 dB lower).

B. Doppler Shift Estimation

In order to recover the data transmitted by the spacecraft during EDL, it is necessary to estimate and correct the Doppler shift of the carrier. Several frequency estimation techniques have been proposed for such purposes. Maximum-likelihood estimation of a single tone embedded in noise is discussed in [7] and [8]. Estimation of signals where the tone frequency changes linearly with time has been studied in the context of chirp signals (see, for example, [9]–[16]). The case where the noise is not additive Gaussian has also been considered in [17] and [18]. In [19], an adaptive algorithm is proposed to track the carrier frequency once it has been acquired. Frequency tracking is also considered in [20]. For the Mars Exploration missions, the technique used is Maximum Likelihood both for carrier acquisition and tracking [5].

In this paper we focus on Maximum Likelihood estimation of the Doppler shift. We address the problem of carrier acquisition, where we need to coarsely estimate the received carrier frequency over a wide bandwidth. We show that improvement over previous methods can be obtained by exploiting (rather than ignoring) the power in the data tones of the transmitted signal to aid the carrier acquisition process. It is shown that the method can provide between 1 and 3 dB improvement, and is suitable for low data-rate, low SNR, and highly dynamic communication systems such as the one used in the Mars exploration missions.

II. Signal Model

We now review the communications system used for the MER missions. As mentioned before, the DTE link uses a special form of MFSK modulation with 8 bits transmitted every 10 s. The models for the transmitted and received signals are described next.

A. Transmitted Signal Model

The signal transmitted from the spacecraft to Earth during the EDL phase has the following form [5]:

$$s(t) = \sqrt{2P_T}\cos\left\{2\pi f_c^0 t + \mu\,\mathrm{Sqr}\left[2\pi \int_{t_0}^{t} f_d(\tau)d\tau\right]\right\}$$

where

- P_T is the transmitted signal power;
- f_c^0 is the nominal carrier frequency;
- μ is the modulation index (typically, $\mu = \pi/4$);
- $\mathrm{Sqr}(x)$ is the limiting function defined by

$$\mathrm{Sqr}(x) = \begin{cases} 1, & 0 < x \le \pi \\ -1, & \pi < x \le 2\pi \end{cases}$$
$$\mathrm{Sqr}(x) = \mathrm{Sqr}\,(x + 2\pi)$$

- $f_d(t)$ is the data tone frequency; it assumes one out of 256 possible values transmitted every 10 s;
- t_0 is the time instant where transmission began (typically, $t_0 \to -\infty$).

B. Received Signal Model

The signal received on Earth during EDL has the following model [5]:

$$r(t) = \sqrt{2P_R(t)}\cos\left\{2\pi \int_{t_0}^{t} f_c(\tau)d\tau + \mu\mathrm{Sqr}\left[2\pi \int_{t_0}^{t} f_d(\tau)d\tau\right]\right\} + v(t) \quad (1)$$

where

- $P_R(t)$ is the time-varying received signal power;
- $f_c(t)$ is the time-varying carrier frequency, which is modeled as

$$f_c(t) = f_c^0 + \Delta f_c(t)$$

where $\Delta f_c(t)$ is the unknown Doppler frequency shift;

- $v(t)$ is a realization of an zero-mean, additive white Gaussian noise wide sense-stationary process with variance σ_v^2.

The signal $r(t)$ is a bandpass signal centered around the frequency f_c^0. It can be expressed in the form

$$\begin{aligned} r(t) &= r_I(t)\cos\left(2\pi f_c^0 t\right) - r_Q(t)\sin\left(2\pi f_c^0 t\right) \\ &= \mathrm{Re}\left\{\tilde{r}(t)e^{j2\pi f_c^0 t}\right\} \end{aligned}$$

where $\tilde{r}(t) = r_I(t) + jr_Q(t)$ is the lowpass equivalent of $r(t)$, and $r_I(t)$ and $r_Q(t)$ are its in-phase and quadrature components. The same relation holds for $v(t)$, namely

$$\begin{aligned} v(t) &= v_I(t)\cos\left(2\pi f_c^0 t\right) - v_Q(t)\sin\left(2\pi f_c^0 t\right) \\ &= \mathrm{Re}\left\{\tilde{v}(t)e^{j2\pi f_c^0 t}\right\}. \end{aligned}$$

The signal $\tilde{v}(t)$ is the low-pass equivalent of $v(t)$, corresponding to a realization of a complex, zero-mean, additive white circular Gaussian noise process of the form $\tilde{v}(t) = v_I(t) + jv_Q(t)$, with $v_I(t)$ and $v_Q(t)$ independent having variance σ_v^2. Note that the variance of $\tilde{v}(t)$ is $\sigma_{\tilde{v}}^2 = 2\sigma_v^2$. The low-pass equivalent of (1) is therefore

$$\begin{aligned} \tilde{r}(t) = \sqrt{2P_R(t)}\exp\Bigg\{ & j\theta + j2\pi\int_{t_0}^{t}\Delta f_c(\tau)d\tau \\ & + j\mu\mathrm{Sqr}\left[2\pi\int_{t_0}^{t} f_d(\tau)d\tau\right]\Bigg\} + \tilde{v}(t) \end{aligned}$$

with $\theta = -2\pi f_c^0 t_0$.

We can express the signal $\tilde{r}(t)$ in discrete-time by sampling at the rate $F_s = 1/T_s$, and using the compact notation $\tilde{r}(n) \triangleq \tilde{r}(nT_s)$ and $\tilde{v}(n) \triangleq \tilde{v}(nT_s)$. Then

$$\boxed{\tilde{r}(n) = A(n)\exp\{j\phi(n)\} + \tilde{v}(n)} \tag{2}$$

where we defined

$$\begin{aligned} A(n) &\triangleq \sqrt{2P_R(nT_s)}e^{j\theta} \\ \phi(n) &\triangleq 2\pi\int_{t_0}^{nT_s}\Delta f_c(\tau)d\tau \\ &\quad + \mu\mathrm{Sqr}\left[2\pi\int_{t_0}^{nT_s} f_d(\tau)d\tau\right]. \end{aligned} \tag{3}$$

Note that if we assume that the data tone frequency is constant $(f_d(t) = f_d)$ between two arbitrary time instants mT_s and $nT_s, n > m$, we have

$$\mathrm{Sqr}\left[2\pi\int_{t_0}^{nT_s} f_d(\tau)d\tau\right] = \mathrm{Sqr}\left(2\pi f_d n/F_s + \varphi\right)$$

where $\varphi = 2\pi[\int_{t_0}^{mT_s} f_d(\tau)d\tau - f_d mT_s]$ is an unknown phase.

Throughout this work, the measure that will be used to quantify the noise level in a signal is the signal-to-noise-PSD ratio [5], and will be denoted by SNR. This measure is defined as the ratio of the received signal power to the white noise power spectral density in dB. Given a noise power spectral density of $\eta/2$, the SNR is defined as

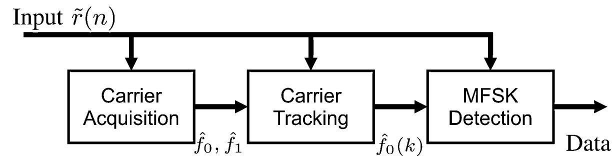

Fig. 3. Carrier acquisition, carrier tracking, and data detection system for MER missions.

$$\mathrm{SNR} = 10\log_{10}\left(\frac{P_R}{\eta/2}\right) = 10\log_{10}\left(\frac{P_R F_s}{\sigma_v^2}\right) \quad [\mathrm{dB-Hz}].$$

Thus the SNR defined in this way has units of Hertz, and in the dB scale this is denoted by dB-Hz. Note that this scale can be converted to conventional SNR by subtracting $10\log_{10}(F_s) = 50$ dB when $F_s = 100$ kHz.

C. Signal Demodulation

The received signal $\tilde{r}(n)$ is demodulated in three stages as shown in Fig. 3. First, a carrier acquisition algorithm is used to obtain a coarse estimate of the Doppler shift and Doppler rate of the received signal. This stage is critical during EDL since all subsequent stages depend on an accurate initial carrier acquisition. The method uses a search over a wide range of possible shifts and rates. After the carrier is acquired, the coarse estimate is refined using a tracking algorithm with a considerably reduced bandwidth. This stage tracks the carrier frequency at a finer scale, and provides carrier estimates for the third block, which performs the MFSK data demodulation.

In this work, we will focus on the carrier acquisition block only, since accurate acquisition is crucial for the subsequent stages. Carrier tracking and demodulation are considered in [5] and [19]. For the carrier acquisition problem, we are interested in coarse estimates of the carrier frequency. The resolution to be used for carrier acquisition is 10 Hz, that is, we need to be able to resolve carrier shifts with an error of ± 5 Hz. As such, our performance metric will not be the mean-square error between the actual and estimated carrier frequency, or the bit error rate at the output of the demodulator, but rather, the probability that we acquire the carrier within the range of ± 5 Hz. A mean-square error measure would be more appropriate for the tracking algorithm, whereas the bit-error rate would be more appropriate for the MFSK demodulation section. Naturally, the probability of carrier acquisition can be translated into a mean-square error measure, but the former measure will be of more interest in our case.

In what follows we will present a method where combining the carrier acquisition stage with the data demodulation stage can lead to a performance improvement of up to 3 dB, a process we denote by *tone demodulation*.

III. Maximum Likelihood Estimation

The objective of the carrier acquisition stage is to estimate the Doppler shift from the received signal $\tilde{r}(n)$ in (2). We will use boldface notation to denote random quantities, and assume that $\tilde{r}(n)$ and $\tilde{v}(n)$ are realizations of the random processes $\tilde{\boldsymbol{r}}(n)$ and $\tilde{\boldsymbol{v}}(n)$, respectively. Then we have

$$\tilde{\boldsymbol{r}}(n) = A(n)e^{j\phi(n)} + \tilde{\boldsymbol{v}}(n)$$

We start by introducing the following assumptions.

- The noise process $\tilde{\boldsymbol{v}}(n)$ is complex, zero-mean, circular Gaussian and iid, with variance $2\sigma_v^2$.
- The data is analyzed in segments of $N \times M$ samples. Typical values are $N = 10000, M = 10$ and $F_s = 100$ kHz, leading to an analysis segment duration of $T = 1$ second. During each segment, the Doppler shift f_0 and rate f_1 are assumed constant, and are modeled as unknown deterministic parameters.
- The complex amplitude $A(n)$ is modeled as a piecewise constant deterministic parameter, i.e., $A(n)$ is assumed constant in intervals of duration N samples, and the amplitude corresponding to the mth segment is denoted by A_m. This assumption is useful to account for multiplicative noise and channel fading, since it allows more frequent changes in the amplitude, compared to less frequent changes in Doppler shift and rate. Furthermore, in order to guarantee an average signal power of $2P_R$ for the low-pass equivalent (2), we require:

$$\frac{1}{M}\sum_{m=0}^{M-1}|A_m|^2 = 2P_R \tag{4}$$

Let $\tilde{\boldsymbol{r}}$ and $\tilde{\boldsymbol{v}}$ denote the random vectors of length NM with individual entries $\tilde{\boldsymbol{r}}(n)$ and $\tilde{\boldsymbol{v}}(n), n = 1, \ldots, NM$, respectively. Under these assumptions, the probability density function (pdf) of the signal $\tilde{\boldsymbol{r}}$ is

$$f_{\tilde{\boldsymbol{r}}}(\tilde{r}(n)) = f_{\tilde{\boldsymbol{v}}}(\tilde{r}(n) - A(n)e^{j\phi(n)}) = \frac{1}{(2\pi\sigma_v^2)^{NM}} \times \exp\left\{-\frac{1}{2\sigma_v^2}\sum_{m=0}^{M-1}\sum_{n=mN}^{mN+N-1}\left|\tilde{r}(n) - A_m e^{j\phi(n)}\right|^2\right\}.$$

By taking the logarithm we arrive at the following log-likelihood function:

$$-\frac{1}{2\sigma_v^2}\sum_{m=0}^{M-1}\sum_{n=mN}^{mN+N-1}|\tilde{r}(n) - A_m e^{j\phi(n)}|^2 - \log(2\pi\sigma_v^2)^{NM}.$$

The Maximum-Likelihood (ML) criterion estimates $\{A_m\}$ and $\phi(n)$ by maximizing the above log-likelihood function, which is equivalent to minimizing the following quadratic form:

$$\min_{\{A_m\},\phi(n)}\sum_{m=0}^{M-1}\sum_{n=mN}^{mN+N-1}|\tilde{r}(n) - A_m e^{j\phi(n)}|^2. \tag{5}$$

Differentiating the above cost with respect to A_m, and setting the result to zero, we get the optimal amplitudes

$$A_m^{\mathrm{opt}} = \frac{1}{N}\sum_{n=mN}^{mN+N-1}\tilde{r}(n)e^{-j\phi(n)}.$$

Substituting this result into (5) we obtain that the original Maximum-Likelihood problem is equivalent to the following maximization problem:

$$\max_{\phi(n)}\sum_{m=0}^{M-1}\left|\sum_{n=mN}^{mN+N-1}\tilde{r}(n)e^{-j\phi(n)}\right|^2. \tag{6}$$

The solution to problem (6) will depend on how we model the unknown phase $\phi(n)$. In general, $\phi(n)$ will be some function of the Doppler frequency shift $\Delta f_c(t)$. This shift can be described using a Taylor series expansion, say

$$\Delta f_c(t) = f_0 + f_1 t + f_2 t^2/2 + \cdots. \tag{7}$$

Thus, by restricting (7) to a few terms, problem (6) becomes a function of a few optimization parameters, as is shown next.

A. Linear Frequency Model

We assume a linear profile for the Doppler shift, and first ignore data tones. The linear profile assumption is reasonable when the length of the data segment to be analyzed is short compared to the change in Doppler frequency. The Doppler shift is modelled as

$$\Delta f_c(t) = f_0 + f_1 t \tag{8}$$

where the Doppler frequency f_0 and Doppler rate f_1 are unknown. Since we are ignoring the data tones, we set $\mu = 0$ in (3) to obtain

$$\phi(n) = 2\pi\left(\frac{f_0 n}{F_s} + \frac{f_1 n^2}{2F_s^2}\right) + \phi_0$$

where ϕ_0 represents some constant phase which depends on t_0. Then the maximization problem (6) becomes

$$\max_{f_0,f_1}\sum_{m=0}^{M-1}\left|\sum_{n=mN}^{mN+N-1}\tilde{r}(n)e^{-j2\pi\left(\frac{f_0 n}{F_s}+\frac{f_1 n^2}{2F_s^2}\right)}\right|^2. \tag{9}$$

This problem is also known as periodogram maximization, and is not convex in general. It is solved typically by searching over a predefined set of possible rates f_1 and frequencies f_0, and then finding the combination that maximizes the expression. Thus, it involves a 2-D grid search, and the finer the grid, the larger the complexity of the search. The method can be extended from the linear case to take into account higher order terms in the expansion (7). For instance, [21] suggests a second-order approximation of the Doppler shift, which leads to a search over f_0, f_1 and f_2.

It is important to note that f_0 and f_1 are continuous parameters, even though the grid search uses a set of discrete search values. The finer the grid, the more likely it will be to find a point close to the actual values.

In what follows we will refer to (9) as *the* ML method, since it is the one currently used in the MER missions. However, it should be kept in mind that the method that follows is also Maximum Likelihood, but with different modeling assumptions.

B. Linear Frequency Model With Data Tones

We now take into account the presence of the data tones in the frequency model, and will show how the combined estimation of the Doppler shift and the data tones leads to performance improvement. The Doppler shift is again assumed to be linear as in (8). When data tones are taken into account in the model for $\phi(n)$ we obtain from (3)

$$\phi(n) = 2\pi\left(\frac{f_0 n}{F_s} + \frac{f_1 n^2}{2F_s^2}\right) + \mu \mathrm{Sqr}\left(\frac{2\pi f_d n}{F_s} + \varphi\right) + \phi_0. \quad (10)$$

Now the ML procedure (6) becomes

$$\max_{f_0, f_1, f_d, \varphi} \sum_{m=0}^{M-1} \left| \sum_{n=mN}^{mN+N-1} \tilde{r}(n) \times e^{-j2\pi\left(\frac{f_0 n}{F_s} + \frac{f_1 n^2}{2F_s^2}\right) - j\mu \mathrm{Sqr}\left(\frac{2\pi f_d n}{F_s} + \varphi\right)} \right|^2 \quad (11)$$

We will refer to (11) as the Maximum Likelihood with Tone Demodulation (MLTD) method. The algorithm typically operates over segments of duration $T = 1$ second ($M = 10, N = 10000$ and $F_s = 100$ kHz). Compared to the ML method (9) without considering data tones, MLTD is more complex because we also have to search over the phases φ and the data tone frequencies f_d. However, as will be discussed later in this section, f_d comes from a discrete set, and in some cases may be known a priori. Also, rough estimates of φ will be sufficient to provide performance improvement.

C. Interpretation of the Tone Demodulation Process

The following interpretation shows why we should expect an improvement of about 3 dB when we take into account the data tones as in (11) over the earlier method (9) where data tones are ignored. The interpretation is included to provide the reader with an intuitive explanation of the process. A more rigorous analysis will be provided in the following section. We will assume, only in this section, that $M = 1$, the Doppler rate $f_1 = 0$ and that the amplitude $A(n) = A$ is constant.

From (2) and (10), the received signal is of the form

$$\tilde{r}(n) = A e^{j\frac{2\pi f_0 n}{F_s} + j\mu\, \mathrm{Sqr}\left(\frac{2\pi f_d n}{F_s} + \varphi\right)} + \tilde{v}(n) \quad (12)$$

with $A = \sqrt{2P_R} e^{j\theta}$. Now note the following:

$$e^{j\mu\, \mathrm{Sqr}\left(\frac{2\pi f_d n}{F_s} + \varphi\right)} = \cos\mu + j\sin\mu \cdot \mathrm{Sqr}\left(\frac{2\pi f_d n}{F_s} + \varphi\right). \quad (13)$$

Consider the Fourier series expansion of the Sqr function:

$$\mathrm{Sqr}\,(2\pi f_d n/F_s + \varphi) = \sum_{k=-\infty}^{\infty} c_k e^{jk\varphi} e^{j2\pi k f_d n/F_s} \quad (14)$$

where

$$c_0 = 0 \text{ and } c_k = \mathrm{sinc}\,(k\pi/2) e^{-jk\pi/2}, k \neq 0.$$

Since $c_k = 0$ for k even, it can be observed that $\tilde{r}(n)$ contains tones at frequencies $f_0, f_0 \pm f_d, f_0 \pm 3f_d, \ldots$. The power of the

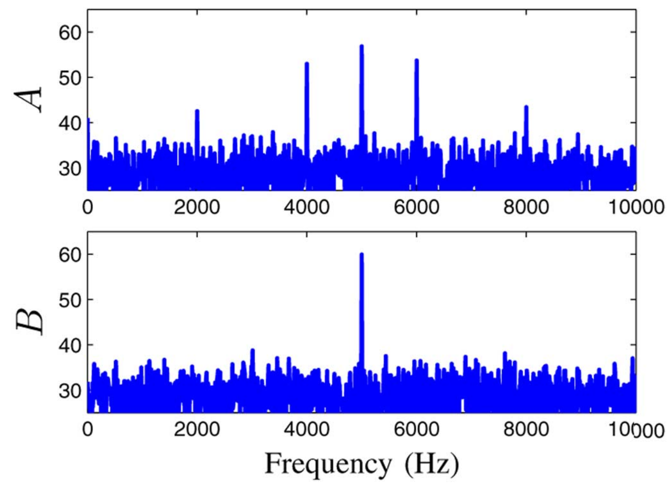

Fig. 4. (A) Magnitude spectrum in dB of received signal, obtained via N point DFT of $\tilde{r}(n)$, using $f_0 = 5000$ Hz, $f_d = 1000$ Hz, SNR=40 dB-Hz and $\mu = \pi/4$. (B) Magnitude spectrum in dB after tone demodulation, obtained via N point DFT of $\tilde{r}(n)e^{-j\mu \mathrm{Sqr}\,(2\pi f_d n/F_s + \varphi)}$.

signal without noise at frequency f_0 is $A^2\cos^2\mu$. The combined power of the two primary subcarriers (at frequencies $f_0 \pm f_d$) is $(8/\pi^2)|A|^2\sin^2\mu$. Fig. 4(a) shows a typical plot of the N point DFT of $\tilde{r}(n)$.

The ML procedure (9) estimates f_0 by demodulating the signal to baseband (multiplying by $e^{-j2\pi f_0 n/F_s}$), and then calculating the sum of the result, obtaining

$$\sum_{n=0}^{N-1} \tilde{r}(n) e^{-j2\pi f_0 n/F_s} = AN\cos\mu + \sum_{n=0}^{N-1} \tilde{v}(n) e^{-j2\pi f_0 n/F_s}.$$

The SNR of this result is

$$\cos^2\mu \times |A|^2 N / \left(2\sigma_v^2\right).$$

On the other hand, we can think of the MLTD procedure (11) as a "tone-demodulation" process followed by the same "signal-demodulation" process as in the ML method. This is accomplished by multiplying by $e^{-j\mu\, \mathrm{Sqr}\,(2\pi f_d n/F_s + \varphi)}$, demodulating to baseband, and taking the sum of the result, to obtain

$$\mathrm{AN} + \sum_{n=0}^{N-1} \tilde{v}(n) e^{-j2\pi f_0 n/F_s - j\mu\, \mathrm{Sqr}\,(2\pi f_d n/F_s + \varphi)}.$$

The SNR of this result is

$$|A|^2 N / \left(2\sigma_v^2\right).$$

We observe that if f_d and φ are appropriately chosen, and using a value of $\mu = \pi/4$, the MLTD method has a SNR enhancement of 3 dB compared to the conventional ML method. The result of the MLTD multiplication causes the data tones to demodulate *onto* the main carrier, and add constructively, therefore enhancing its power and allowing better estimation performance [see Fig. 4(b)]. Since about half of the power is in the carrier and the remainder in the data tones, a 3 dB enhancement of the carrier power is expected.

D. Complexity of the Tone Demodulation Process

The ML method (9) requires a search over N_{f_0} and N_{f_1} discrete frequencies f_0 and f_1, respectively, whereas the MLTD method (11) requires searching also over N_{f_d} and N_φ discrete values of f_d and φ, respectively. Using typical values of $N = N_{f_0} = 10000, N_{f_1} = 57, N_{f_d} = 256, N_\varphi = 8$ and $M = 10$ (see Section IV), MLTD requires on the order of $MN_{f_1}N_{f_d}N_\varphi N_{f_0} \log N_{f_0}$ floating point operations. Moreover, MLTD is roughly 1000 more complex than ML in its general form. However, when f_d is known, MLTD is only eight times more complex than ML, and provides significant performance improvement. In general f_d is unknown, but since this frequency is kept constant for every 10 segments, the value may be known from a previous segment estimate. When f_d is unknown, the method is still useful, since it can be applied only to those segments of the signal which are extremely noisy, and where the original ML method performs poorly.

Also, note that if we approximate (14) by its first harmonic

$$e^{j\mu \,\mathrm{Sqr}\left(\frac{2\pi f_d n}{F_s}+\varphi\right)} \approx \cos\mu + j\sin\mu\left(c_1 e^{j\left(\frac{2\pi f_d n}{F_s}+\varphi\right)} - c_{-1}e^{-j\left(\frac{2\pi f_d n}{F_s}+\varphi\right)}\right)$$

then we need not take a new DFT for every value of f_d and φ, but rather replace them by shifts and additions of the same spectrum. If we can do shifts and additions efficiently, we can reduce the complexity of MLTD to that of ML, at the expense of some performance hit due to the above approximation.

IV. Performance Analysis

We now analyze the performance of the MLTD estimation method. The analysis can be extended to the case where the Doppler shift is assumed to include higher order terms of the expansion (7). The following analysis extends the results of [5] to the more general case (11) when data tones are taken into account rather than ignored.

A. Signal Model and Performance Metric

It is assumed that the received signal has the form (12), with a piecewise-constant amplitude as discussed in Section III, and that the data tone frequency is fixed at f_d. The signal is analyzed in segments of duration T seconds, where $T = MN/F_s$. We use the notation f_0, f_1, f_d and φ to refer to the *true* parameters of the received signal. The MLTD method of (11) requires multiplying $\tilde{r}(n)$ by

$$d(n;\theta) \triangleq e^{-j2\pi\left(\frac{f_0' n}{F_s}+\frac{f_1' n^2}{2F_s^2}\right)-j\mu\,\mathrm{Sqr}\left(\frac{2\pi f_d' n}{F_s}+\varphi'\right)}$$

where we have introduced the notation f_0', f_1', f_d' and φ' to refer to the *dummy* search variables, and where θ denotes a vector of search parameters ordered as follows:

$$\theta = [f_0'\ f_1'\ f_d'\ \varphi']$$

The ML estimates of f_0, f_1, f_d and φ are found by solving

$$\{\hat{f}_0, \hat{f}_1, \hat{f}_d, \hat{\varphi}\} = \arg\max_{f_0' f_1' f_d' \varphi'} J(\tilde{r}(n);\theta) \tag{15}$$

with

$$J(\tilde{r}(n);\theta) \triangleq \sum_{m=0}^{M-1}\left|\sum_{n=mN}^{mN+N-1}\tilde{r}(n)d(n;\theta)\right|^2. \tag{16}$$

The cost $J(\tilde{r}(n);\theta)$ is a realization of a real, scalar random variable $\boldsymbol{J}(\tilde{\boldsymbol{r}}(n);\theta)$ whose distribution depends on the parameters f_0', f_1', f_d' and φ'. Once $\tilde{r}(n)$ is received, we compute the deterministic cost J, and the ML method selects the set of parameters that maximize J.

To make the analysis tractable, we introduce some simplifying assumptions. Define the auxiliary function

$$g_m(x(n)) \triangleq \sum_{n=mN}^{mN+N-1} e^{j2\pi x(n)n}. \tag{17}$$

When the argument of g_m is equal to a constant k/N, we get

$$g_m(k/N) = g_0(k/N) = \begin{cases} N, & k = rN, r \in \mathbb{Z} \\ 0, & \text{otherwise} \end{cases}$$

We assume that:

- $f_0 = kF_s/N$ for some integer k. This assumption is not true in practice, since f_0 is a continuous variable. The farther f_0 is from a multiple of kF_s/N, the worse our estimate will be. However, since this problem will affect in the same manner the proposed MLTD method and the original ML method, we will assume in our calculations that this assumption holds. Typically, we will have $N/F_s = 0.1$ sec, so f_0 will be considered a multiple of 10 Hz. Thus, the search will be performed at integer multiples of F_s/N, that is, $f_0' = k'F_s/N$ for some integer k'. Since we are free to choose the tone frequencies f_d, we will also assume $f_d = kF_s/N$ for some integer $k \neq 0$
- $g_m(\Delta f_1 n/(2F_s^2) + k/N) \approx 0$ if $\Delta f_1 \neq 0$, for any integer k. This result is also not true in general, but the approximation is good for values Δf_1 large enough. As we decrease the value of Δf_1, the probability of making an error by selecting a grid point close to the true one increases, but so does the frequency resolution. Moreover, we are mostly interested in estimating the Doppler shift f_0, since we assume a carrier tracking stage follows, which reduces the search range around the estimated frequency f_0. Hence small errors in detecting f_1 are not of major concern as long as f_0 is acquired correctly.

The metric used to evaluate the performance of the algorithm is the probability of error in carrier acquisition, P_e, defined as the probability that the estimate $\hat{f}_0$ is different from the true value f_0. In terms of $\boldsymbol{J}$, it can be expressed as follows:

$$P_e = \mathrm{Prob}\left\{\boldsymbol{J}(\tilde{\boldsymbol{r}}(n);\theta') \geq \boldsymbol{J}(\tilde{\boldsymbol{r}}(n);\theta'')\right\} \tag{18}$$

for *at least* one set of values of $\theta' = [f_0'\ f_1'\ f_d'\ \varphi']$ such that $f_0' \neq f_0$, and for *every* value of $\theta'' = [f_0\ f_1''\ f_d''\ \varphi'']$.

To derive expressions for P_e, we will proceed as follows. For every combination of values of the parameters f_0', f_1', f_d' and φ', we will derive an expression for the probability distribution of the resulting random variable $\boldsymbol{J}$. Subsequently, we will compute P_e from (18).

B. Statistics of the Estimates

Define the differences $\Delta f_0 \triangleq f_0 - f_0'$, $\Delta f_1 \triangleq f_1 - f_1'$, $\Delta f_d \triangleq f_d - f_d'$, $\Delta\varphi \triangleq \varphi - \varphi'$. It then follows that

$$\begin{aligned}\tilde{\boldsymbol{r}}(n)d(n;\theta) = A(n)\exp\Bigg\{ & j2\pi\left(\frac{\Delta f_0 n}{F_s} + \frac{\Delta f_1 n^2}{2F_s^2}\right) \\ & + j\mu \,\mathrm{Sqr}\left(2\pi\frac{f_d}{F_s}n + \varphi\right) \\ & - j\mu \mathrm{Sqr}\left(2\pi\frac{f_d'}{F_s}n + \varphi'\right)\Bigg\} + \tilde{\boldsymbol{v}}(n)d(n;\theta).\end{aligned} \tag{19}$$

From (13), we have

$$\begin{aligned} & e^{j\mu\left[\mathrm{Sqr}\left(\frac{2\pi f_d n}{F_s}+\varphi\right) - \mathrm{Sqr}\left(\frac{2\pi f_d' n}{F_s}+\varphi'\right)\right]} = \cos^2\mu \\ & + j\sin\mu\cos\mu\cdot\left[\mathrm{Sqr}\left(\frac{2\pi f_d n}{F_s}+\varphi\right)\right. \\ & \left. - \mathrm{Sqr}\left(\frac{2\pi f_d' n}{F_s}+\varphi'\right)\right] \\ & + \sin^2\mu\cdot\,\mathrm{Sqr}\left(\frac{2\pi f_d n}{F_s}+\varphi\right)\mathrm{Sqr}\left(\frac{2\pi f_d' n}{F_s}+\varphi'\right).\end{aligned} \tag{20}$$

We also introduce the following useful notation:

$$\begin{aligned}\boldsymbol{R}_m &\triangleq \sum_{n=mN}^{mN+N-1} \tilde{\boldsymbol{r}}(n)d(n;\theta) \\ \boldsymbol{V}_m &\triangleq \sum_{n=mN}^{mN+N-1} \tilde{\boldsymbol{v}}(n)d(n;\theta) \\ \boldsymbol{R}_m &= T_m + \boldsymbol{V}_m.\end{aligned}$$

Using (19), (20), (17), and (14), we arrive at

$$\begin{aligned} T_m = {} & A_m\cos^2\mu\cdot g_m\left(\frac{\Delta f_0}{F_s} + \frac{\Delta f_1 n}{2F_s^2}\right) \\ & + jA_m\sin\mu\cos\mu\sum_k c_k e^{jk\varphi} g_m \\ & \times\left(\frac{\Delta f_0 + k f_d}{F_s} + \frac{\Delta f_1 n}{2F_s^2}\right) \\ & - jA_m\sin\mu\cos\mu\sum_k c_k e^{jk\varphi'} g_m \\ & \times\left(\frac{\Delta f_0 + k f_d'}{F_s} + \frac{\Delta f_1 n}{2F_s^2}\right) \\ & + A_m\sin^2\mu\sum_k\sum_l c_k c_l e^{j(k\varphi + l\varphi')} g_m \\ & \times\left(\frac{\Delta f_0 + k f_d + l f_d'}{F_s} + \frac{\Delta f_1 n}{2F_s^2}\right)\end{aligned} \tag{21}$$

Equation (21) is important for our analysis, since it allows us to find an expression for statistics of $\boldsymbol{R}_m$ for every value of search parameters f_0', f_1', f_d' and φ' as a function of the true parameters f_0, f_1, f_d and φ.

Note that $\boldsymbol{V}_m$ is a zero-mean, complex Gaussian random variable with variance $2N\sigma_v^2$, independent of $\boldsymbol{V}_n$ for $m \neq n$. Therefore, we have that

$$\frac{1}{2N\sigma_v^2}\boldsymbol{J}(\tilde{\boldsymbol{r}}(n;\theta)) = \frac{1}{2N\sigma_v^2}\sum_{m=0}^{M-1}|\boldsymbol{R}_m|^2 \sim \chi^2_{2M,\lambda}$$

where $\chi^2_{2M,\lambda}$ represents a noncentral chi-square distribution with $2M$ degrees of freedom and noncentrality parameter

$$\lambda = \frac{1}{N\sigma_v^2}\sum_{m=0}^{M-1}|T_m|^2. \tag{22}$$

The pdf of $\boldsymbol{X} \sim \chi^2_{2M,\lambda}$ is (for $x \geq 0, \lambda_i \neq 0$)

$$f_{\boldsymbol{X}}(x) = \frac{e^{-(x+\lambda)/2}}{2}\left(\frac{x}{\lambda}\right)^{\frac{M-1}{2}} I_{M-1}(\sqrt{\lambda x}) \tag{23}$$

where $I_n(x)$ is the modified Bessel function of the first kind. When $\lambda = 0, \boldsymbol{X}$ is distributed according to a central chi-square distribution. In this case, the pdf becomes (for $x \geq 0$)

$$f_{\boldsymbol{X}}(x) = \frac{e^{-x/2}x^{M-1}}{2^M(M-1)!}. \tag{24}$$

C. Parameter Classes and Probability of Error

In our search procedure we will search over $N_{f_0}, N_{f_1}, N_{f_d}$ and N_φ discrete values of f_0', f_1', f_d' and φ', respectively. Let $\mathcal{M}_\theta \in \mathbb{R}^{N_{f_0}\times N_{f_1}\times N_{f_d}\times N_\varphi}$ denote the space of all possible search vectors θ. We will partition this space as follows.

$$\begin{aligned} & \mathcal{P}_1 : \{\theta : f_0' = f_0, f_1' = f_1, f_d' = f_d\} \\ & \mathcal{P}_2 : \{\theta : f_0' = \pm f_d, f_1' = f_1, f_d' = f_d\} \\ & \mathcal{P}_3 : \{\theta : f_0' = \pm 2f_d, f_1' = f_1, f_d' = f_d\} \\ & \mathcal{P}_4 : \{\theta : f_0' = f_0, f_1' = f_1, f_d' \neq f_d\} \\ & \mathcal{P}_5 : \{\theta : f_0' = \pm f_d, \pm f_d', f_1' = f_1, f_d' \neq f_d\} \\ & \mathcal{P}_6 : \{\theta : f_0' = \pm(f_d + f_d'), \\ & \quad \pm(f_d - f_d'), f_1' = f_1, f_d' \neq f_d\} \\ & \mathcal{P}_0 : \{\theta : \theta \notin \{\cup_{i=1}^6 \mathcal{C}_i\}\}.\end{aligned}$$

When f_d is known, only partitions 0 to 3 exist. Whenever θ belongs to $\mathcal{P}_1$ or $\mathcal{P}_4$, the value of f_0' will be equal to the true value f_0. For every partition, we define a set of identically distributed random variables

$$\boldsymbol{X}_i(\theta) = \frac{1}{2N\sigma_v^2}\boldsymbol{J}(\tilde{\boldsymbol{r}}(n);\theta\in\mathcal{P}_i) \sim \chi^2_{2_M,\lambda_i}.$$

Using (21) and (22), and using the relation $2\mathrm{SNR}\times T = 2P_R^{MN}/\sigma_v^2$, we obtain

$$\begin{aligned}\lambda_0 &= 0 \\ \lambda_1 &= 2\mathrm{SNR}\times T\times[\cos^2\mu + \sin^2\mu\cdot(1 - 2|\Delta\varphi|/\pi)]^2 \\ \lambda_2 &= 2\mathrm{SNR}\times T\times\frac{8}{\pi^2}\sin^2\mu\cos^2\mu(1-\cos\Delta\varphi) \\ \lambda_3 &= 2\mathrm{SNR}\times T\times\frac{4}{\pi^2}\sin^4\mu\sin^2\Delta\varphi \\ \lambda_4 &= 2\mathrm{SNR}\times T\times\cos^4\mu\end{aligned}$$

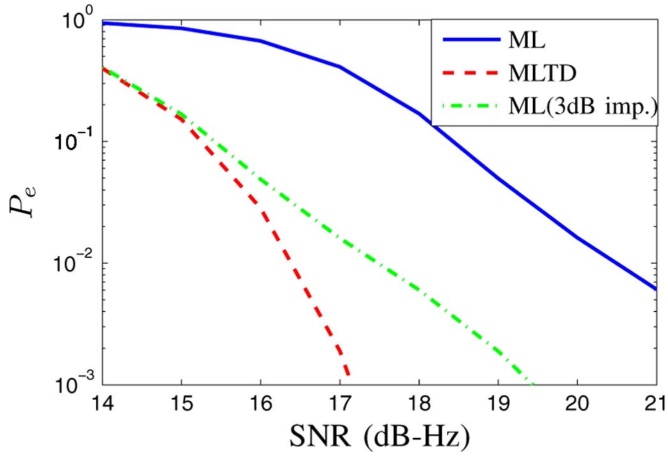

Fig. 5. Probability of error in carrier acquisition vs. SNR for $\Delta\varphi = 0, \Delta f_d = 0$. (Continuous line) ML method. (Dashed line) MLTD. (Dot-dashed line) 3-dB improvement over ML method.

$$\lambda_5 = 2\text{SNR} \times T \times \frac{4}{\pi^2} \sin^2 \mu \cos^2 \mu$$
$$\lambda_6 = 2\text{SNR} \times T \times \frac{16}{\pi^4} \sin^4 \mu. \tag{25}$$

A more detailed derivation can be found in the Appendix. We also define

$$\boldsymbol{Y}_i = \max_{\theta \in \mathcal{P}_i} \boldsymbol{X}_i(\theta).$$

Thus, the probability of error can now be rewritten as

$$P_e = \text{Prob}\left(\max(\boldsymbol{Y}_0, \boldsymbol{Y}_2, \boldsymbol{Y}_3, \boldsymbol{Y}_5, \boldsymbol{Y}_6) > \max(\boldsymbol{Y}_1, \boldsymbol{Y}_4)\right)$$
$$\approx \text{Prob}(\max(\boldsymbol{Y}_0, \boldsymbol{Y}_2, \boldsymbol{Y}_3, \boldsymbol{Y}_5, \boldsymbol{Y}_6) > \boldsymbol{Y}_1)$$

where the last approximation follows from the fact that the probability of $\boldsymbol{Y}_1 > \boldsymbol{Y}_4$ is high. We will evaluate P_e in three scenarios: when f_d and φ are known, when only f_d is known, and when all the parameters are unknown.

1) Known f_d and φ: When f_d and φ are known, the parameter space $\mathcal{M}_\theta$ is partitioned in four classes. Class $\mathcal{P}_1$ has one element, classes $\mathcal{P}_2$ and $\mathcal{P}_3$ have two elements each, and class $\mathcal{P}_0$ has $N_{f_0}N_{f_1} - 5$ elements. Moreover, $\boldsymbol{V}_m(\theta_1)$ and $\boldsymbol{V}_m(\theta_2)$ are uncorrelated (and therefore also independent) whenever θ_1 and θ_2 are in different classes. This means that the $\boldsymbol{X}_i(\theta_j)$ are independent in i and j. Let $f_{\boldsymbol{X}_i}$ and $F_{\boldsymbol{X}_i}$ denote the probability density function and cumulative density function, respectively, of the random variable $\boldsymbol{X}_i$. Since all random variables $\boldsymbol{Y}_i$ are also independent, we have that the probability of correct carrier acquisition $P_{\text{acq}} = 1 - P_e$ is

$$P_{\text{acq}} = \int_0^{+\infty} F_{\boldsymbol{X}_2}^2 F_{\boldsymbol{X}_3}^2 F_{\boldsymbol{X}_0}^{N_{f_1}N_{f_0}-5} f_{\boldsymbol{X}_1}(x)dx$$
$$\approx \int_0^{+\infty} F_{\boldsymbol{X}_0}^{N_{f_1}N_{f_0}-5}(x) f_{\boldsymbol{X}_1}(x)dx. \tag{26}$$

Fig. 5 shows the probability of error in carrier acquisition, P_e versus the SNR for the ML method without tone demodulation (ML) and with tone demodulation (MLTD) using expression (26) where $\Delta\varphi = 0$ and f_d is known. We have chosen the values $N_{f_0} = 10000$ and $N_{f_1} = 57$ as in [5]. The curve for ML is the same one reported in [5]. Also shown is a 3 dB-improvement curve of ML. We can clearly see that MLTD achieves 3-dB improvement for low values of SNR, and even better improvement for high values of SNR. Though a 3-dB improvement is expected, more than that is surprising. The reason is that in the ML curve, the performance at high values of SNR is limited by the presence of the primary data tones at $f_c + f_d$ and $f_c - f_d$. When we apply tone demodulation, not only we double the power of the carrier at f_c, obtaining a 3-dB improvement, but we also eliminate the data tones at frequencies $f_c + f_d$ and $f_c - f_d$ (see Fig. 4). Thus, the improvement is larger than 3 dB for high SNR. This is the most optimistic scenario, where φ and f_d are known. Though in practice we may have knowledge of f_d, we will never know exactly what φ is. We will consider the effect of these parameters next.

2) Known f_d: The maximization procedure (15) requires searching over N_φ phases φ'. We propose searching over a set of phases uniformly distributed between 0 and 2π. Analyzing exactly the performance of this method is challenging, because we now deal with chi-square random variables that come from highly correlated Gaussians. We tackle the problem by simulating the problem using artificial data, and then making some reasonable assumptions that let us obtain expressions that closely agree with the simulation results. Thus, we propose the following assumptions when $\Delta f_d = 0$.

Note that if we search over uniformly distributed phases φ', the maximum difference $\Delta\varphi$ between φ and the closest φ' will be π/N_φ. Since the actual phase φ can be anywhere between 0 and 2π, the expected value of $|\Delta\varphi|$ will be $\pi/(2N_\varphi)$. We will assume that the random variables $\boldsymbol{Y}_1, \boldsymbol{Y}_2$ and $\boldsymbol{Y}_3$ have the same distribution as $\boldsymbol{X}_1(\theta), \boldsymbol{X}_2(\theta)$ and $\boldsymbol{X}_3(\theta)$ respectively, using values λ_i obtained using $\Delta\varphi = \pi/(2N_\varphi)$, and also assume them independent as before. For $\boldsymbol{Y}_0$, we will assume that all variables $\boldsymbol{X}_0(\theta), \theta \in \mathcal{P}_0$ are independent. Then we can compute P_{acq} as follows:

$$P_{acq} \approx \int_0^{+\infty} F_{\boldsymbol{X}_2}^2 F_{\boldsymbol{X}_3}^2 F_{\boldsymbol{X}_0}^{(N_{f_1}N_{f_0}-5)N_\varphi} f_{\boldsymbol{X}_1}(x)dx$$
$$\approx \int_0^{+\infty} F_{\boldsymbol{X}_0}^{(N_{f_1}N_{f_0}-5)N_\varphi}(x) f_{\boldsymbol{X}_1}(x)dx. \tag{27}$$

Note that (27) is a generalization of (26) for the case $N_\varphi \neq 1$.

Fig. 6 shows the resulting curves obtained using expression (27) for the case when f_d is known, with $N_{f_0} = 10000$ and $N_{f_1} = 57$. We can observe that there is practically no gain in increasing the search range from 8 to 16 phases. Hence, we propose the following search procedure for φ: search over 8 values of φ' uniformly distributed between 0 and 2π, and choose the phase φ' that maximizes (15). In Section V, we compare the predicted curves with the results obtained using artificially generated data.

3) All Parameters Unknown: The performance curve also depends on the number of possible data tone frequencies, N_{f_d}. The best scenario occurs when the tone frequency is known, in which case we have $N_{f_d} = 1$. When f_d is unknown, the fact that the random variables $\boldsymbol{X}_i(\theta)$ are heavily correlated makes the analysis challenging. As we did in Section IV-C.2, we will

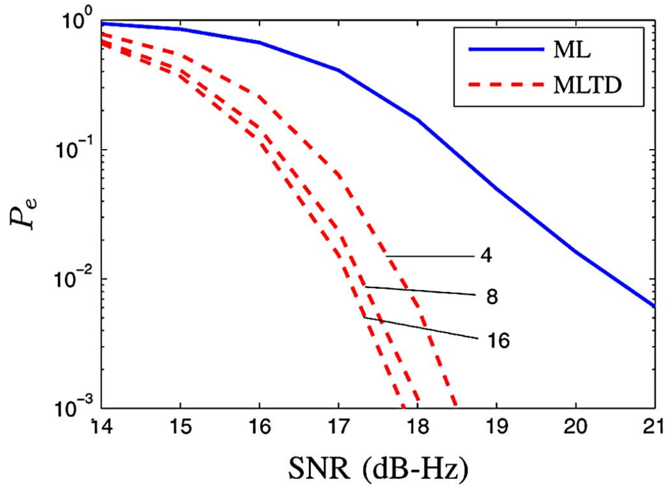

Fig. 6. Probability of error in carrier acquisition vs. SNR for $\Delta f_d = 0$, and using search with different values of N_φ. (Continuous line) ML method. (Dashed line) MLTD for $N_\varphi = 16, N_\varphi = 8$ and $N_\varphi = 4$.

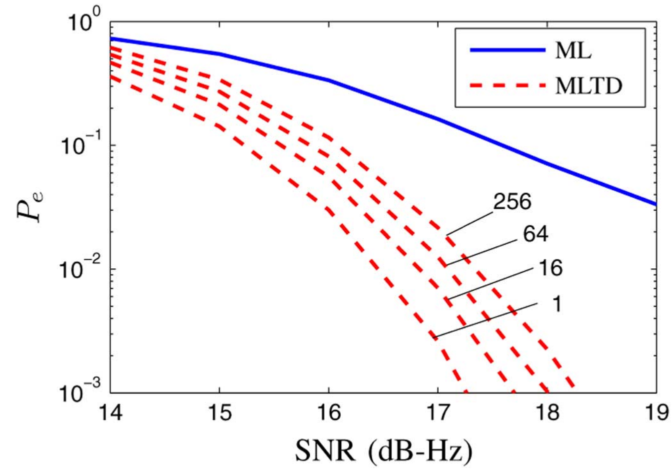

Fig. 7. Probability of error in carrier acquisition versus SNR for $\Delta\varphi = 0$, and different number of possible values for the data tones N_{f_d}. (Continuous line) ML method. (Dashed line) MLTD: 1, 16, 64, and 256 data tones.

approximate the performance curves using heuristics, and illustrate the results using simulations. Again we will approximate $\boldsymbol{Y}_1, \boldsymbol{Y}_2$ and $\boldsymbol{Y}_3$ by $\boldsymbol{X}_1(\theta), \boldsymbol{X}_2(\theta)$ and $\boldsymbol{X}_3(\theta)$, respectively, using $\Delta\varphi = \pi/(2N_\varphi)$. For $\boldsymbol{Y}_0, \boldsymbol{Y}_5$ and $\boldsymbol{Y}_6$, we will assume that $\boldsymbol{X}_0(\theta), \boldsymbol{X}_5(\theta)$ and $\boldsymbol{X}_6(\theta)$ of the form $\boldsymbol{X}_i(\theta_j)$ are independent in i and j, but modify the number of independent random variables by replacing N_{f_d} by $N'_{f_d} = \lfloor N_{f_d}/(1+\log_2 N_{f_d})\rfloor$. Then we can compute P_{acq} as follows:

$$P_{acq} \approx \int_0^{+\infty} F^2_{\boldsymbol{X}_2} F^2_{\boldsymbol{X}_3} F^{N'_5}_{\boldsymbol{X}_5} F^{N'_6}_{\boldsymbol{X}_6} F^{N'_0}_{\boldsymbol{X}_0} f_{\boldsymbol{X}_1}(x)dx \approx \int_0^{+\infty} F^{N'_5}_{\boldsymbol{X}_5}(x) F^{N'_0}_{\boldsymbol{X}_0}(x) f_{\boldsymbol{X}_1}(x)dx \quad (28)$$

with

$$N'_5 = N'_6 = (4N'_{f_d} - 4)N_\varphi$$
$$N'_0 = N_{f_1} N'_{f_d} N_{f_0} N_\varphi - 9N'_{f_d} N_\varphi + 4N_\varphi$$
$$N'_{f_d} = \lfloor N_{f_d}/(1+\log_2 N_{f_d})\rfloor.$$

Note that (28) is more general than (27), since for $N_{f_d} = 1$ we get $N'_{f_d} = 1$.

Fig. 7 shows the effect of N_{f_d} on performance. The curves were obtained using (28), with $N_{f_0} = 10000, N_{f_1} = 57, N_\varphi = 8$ and $\Delta\varphi = \pi/(2N_\varphi)$. As expected, as we increase the possible number of tone frequencies, the performance becomes worse, but even for large N_{f_d}, we have performance improvement over the case where the tones are ignored.

V. Simulations

We now show simulation results that illustrate the performance analysis of the previous sections. We simulate the method using both artificial data generated according to model (12) and real data from the 2004 MER mission.

A. Artificial Data

Artificial Data was generated according to model (12), assuming a linear frequency shift. The sampling frequency was chosen as $F_s = 50$ kHz, and $N = N_{f_0} = 5000$. The Doppler rate, f_1, was also assumed to be known, and therefore $N_{f_1} = 1$. Although this is not true in general, we expect the performance of both methods, ML and MLTD to be degraded in the same amount when f_1 is unknown. We first consider the case where the data tone frequency f_d is known and then the more general case where it is unknown.

1) Known f_d: To analyze the performance of the method when f_d is known, artificial data was generated with different values of SNR, and 1000 experiments were performed. Both the traditional ML method (9) and the MLTD method (11) were implemented. The initial phase φ of the signal was chosen at random at the beginning of every experiment.

Fig. 8 shows the resulting probability of error in carrier acquisition vs. SNR for the ML and MLTD methods, searching over a different number of phases φ'. All searches use N_φ phases uniformly distributed between 0 and 2π. For every value of SNR, the probability of error was calculated using 1000 experiments. We can clearly see that for $N_\varphi = 16$, the performance is slightly better than the one with the choice $N_\varphi = 8$. Hence, we conclude that it is not worth to search over 16 phases due to its increased computational burden and negligible improvement. We suggest a value of $N_\varphi = 8$ for the phase search. Also shown are the predicted curves for ML from [5] and MLTD using expression (27), which very closely match the simulation results.

2) Unknown f_d: We now drop the assumption that f_d is known. We still assume that f_1 is known to reduce the number of computations, and expect the performance to be equally degraded for both ML and MLTD when this is not true.

Fig. 9 shows the resulting performance curves when both f_d and φ are unknown, with $N_{f_d} = 256$ and $N_\varphi = 8$. For every value of SNR, the probability of error was computed using 100 experiments. Also shown are the predicted curves for ML in [5] and MLTD using (28).

B. Real Data

We now present simulation results for the ML-TD method using real data from the 2004 Mars Exploration Rover (MERB)

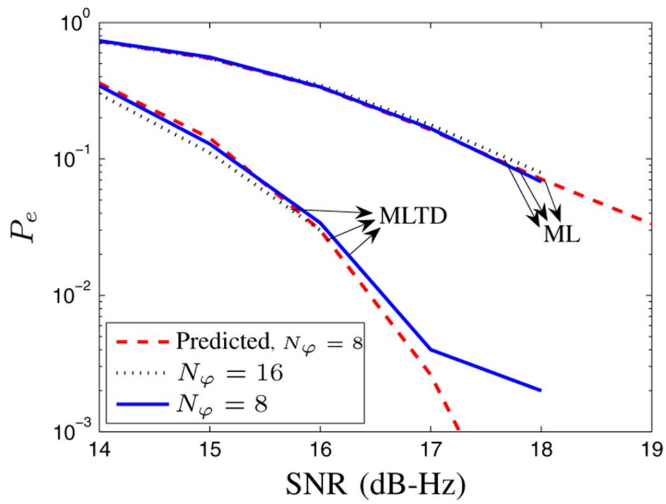

Fig. 8. Results obtained for ML and MLTD using artificial data, f_d known. (Continuous line) Predicted results using 8 phases. (Dashed line) Search using 16 phases. (Dotted line) Search using eight phases.

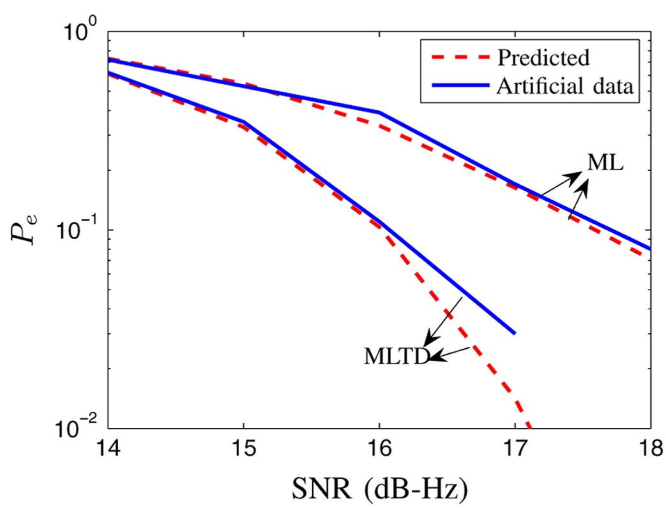

Fig. 9. Results obtained for ML and MLTD using artificial data, f_d unknown. (Continuous line) Results using artificial data. (Dashed line) Predicted results.

mission. The simulations were performed by choosing a segment of the real data where the frequency profile does not resemble a linear curve, and second derivatives of the Doppler shift may be important. The original segment was processed using the original ML method to extract f_0 and f_1, and its SNR was predicted. Subsequently, artificially generated noise was added to take the SNR to the desired levels. As was done previously, f_1 was assumed to be known in all cases to reduce computations. Since the sampling frequency of the MERB data is 100 kHz, we decimated by a factor of 2 to obtain data sampled at 50 kHz. As we did for the artificial data, we chose $N_{f_0} = 5000$ and $N_{f_1} = 1$.

1) Known f_d: Fig. 10 shows the performance curves obtained with the real data when f_d is known. Also shown for comparison are the curves obtained using the performance analysis of the previous section. For every value of SNR, 1000 experiments were performed for the probability calculations.

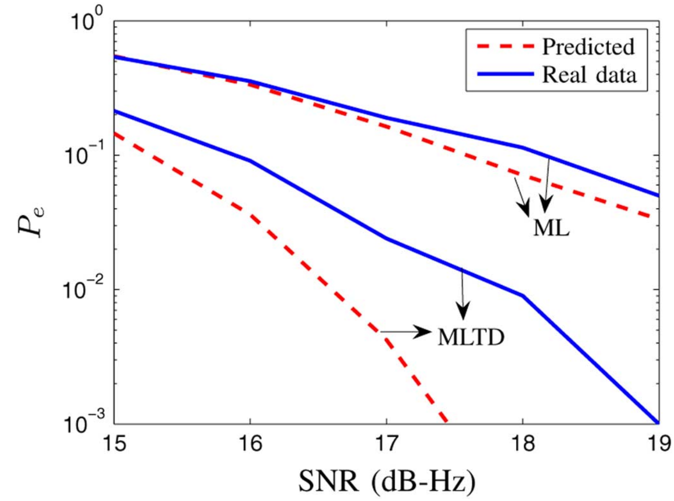

Fig. 10. Results obtained for ML and MLTD using real MERB data, f_d known, $N_\varphi = 8$. (Continuous line) Results using real data. (Dashed line) Predicted results.

The difference between the actual and predicted curves can be attributed to several phenomena. First and foremost, the performance curves were derived for the linear frequency model, and thus are in concordance with the artificially generated data. The real data, however, does not offer a perfectly linear profile. The performance may be improved by also estimating second derivatives of Doppler shift. A second reason for the difference between the curves lies in the estimation of the SNR of the original data before adding noise. This estimate was obtained by finding the peak-power to noise-floor ratio, after applying the original ML method.

Much more interesting and relevant is the fact that the MLTD method preserves a 2- to 3-dB advantage over the original ML method.

2) Unknown f_d: Fig. 11 shows the performance curves obtained with the real data when f_d is not known. Also shown for comparison are the curves obtained using the performance analysis of the previous section. For every value of SNR, 100 experiments were performed for the probability calculations.

The reasons for difference between predicted and actual curves from the case when f_d is known still apply. We can clearly observe that MLTD preserves a 1-dB improvement over the original ML method.

VI. Discussion

The proposed method is shown to provide about 3-dB improvement both for artificially generated data and real data, when the tone frequency f_d is known. Though this is not true in general, the case where f_d is known is relevant in practice. For the MER communications system, as discussed previously, f_d is kept constant for 10 s, and the carrier is estimated for every 1 s. Therefore, we could use the value of f_d obtained on a previous segment to estimate the carrier in the current segment. Moreover, during EDL there exists a most-likely sequence of tones which may be used for detection.

When f_d is unknown, we have to resort to extensive search methods, which are computationally intensive. However, it is not necessary to apply them at every point of the signal. That is,

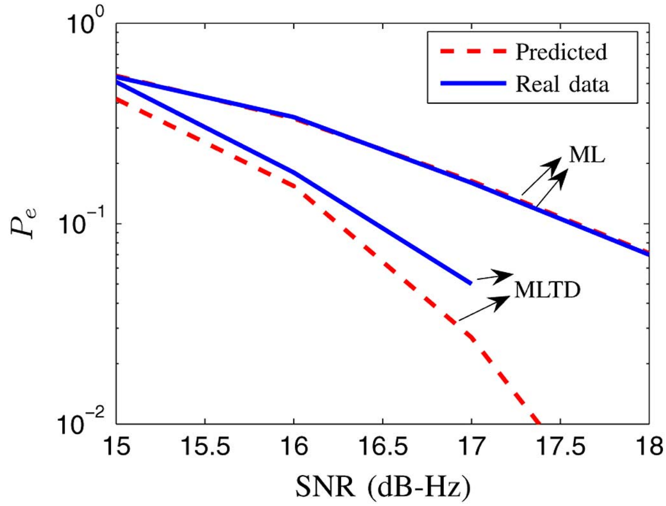

Fig. 11. Results obtained for ML and MLTD using real MERB data, f_d unknown, $N_\varphi = 8$. (Continuous line) Results using real data. (Dashed line) Predicted results.

the original ML method could be applied on a first pass over the entire signal, and then MLTD could be applied over the segments with low predicted SNR. Another alternative is the shifting approach of Section III-D. We have also shown that a search over eight different values of φ' is sufficient to obtain good results.

Finally, one could consider modifying the communications signal for the method to have better performance when f_d is unknown. For instance, instead of sending one out of 256 tones every 10 s, we could send one out of 16 tones every 5 s s. We would be decreasing redundancy, but this would considerably aid the search process, providing much lower computational burden, and better performance.

VII. Conclusion

We presented a ML estimation algorithm to perform carrier frequency estimation for the communications system of the Mars Exploration missions. The method utilizes the power in the data tones to enhance the carrier, enabling in theory more than 3-dB improvement. We analyzed the performance of the method and simulated it using artificially generated data. Finally, we tested the algorithm on the signal obtained during the MERB mission, showing that a 2- to 3-dB improvement may be possible when the data tone frequency is known, and a 1-dB improvement when it is unknown.

Appendix
Derivation of (25)

Whenever $f_1' \neq f_1$, or equivalently $\Delta f_1 \neq 0$, we have $\boldsymbol{R}_m = \boldsymbol{V}_m$ and therefore $\lambda_0 = 0$. When $\Delta f_1 = 0$, we have from (21)

$$T_m = A_m \cos^2\mu \cdot g_0\left(\frac{\Delta f_0}{F_s}\right)$$

$$+ jA_m \sin\mu\cos\mu \sum_k c_k e^{jk\varphi} g_0\left(\frac{\Delta f_0}{F_s} + \frac{kf_d}{Fs}\right)$$
$$- jA_m \sin\mu\cos\mu \sum_k c_k e^{jk\varphi'} g_0\left(\frac{\Delta f_0}{F_s} + \frac{kf_d'}{Fs}\right)$$
$$+ A_m \sin^2\mu \sum_k\sum_l c_k c_l e^{j(k\varphi + l\varphi')} g_0$$
$$\times\left(\frac{\Delta f_0}{F_s} + \frac{kf_d + lf_d'}{F_s}\right). \tag{29}$$

Without loss of generality, we will consider values of $\Delta\varphi$ in the interval $[-\pi, \pi]$. When $\Delta f_d = 0$ and $\Delta f_0 = lf_d, l \in \mathbb{Z}$, the fifth term in (29) is equal to

$$A_m N \sin^2\mu\left[\delta(l) - \frac{4}{l\pi} e^{j\frac{l}{2}(\varphi+\varphi'-\pi)}\cos\left(\frac{l\pi}{2}\right)\sin\left(\frac{l\Delta\varphi}{2}\right)\right]$$
$$= \begin{cases} 0, & l \text{ odd} \\ A_m N\sin^2\mu\left(1 - \frac{2}{\pi}|\Delta\varphi|\right), & l = 0 \\ -A_m N \sin^2\mu\frac{2}{\pi}e^{\mp j(\varphi+\varphi')}\sin|\Delta\varphi|, & l = \pm 2 \end{cases}.$$

We are now in a position to find the values of T_m for different scenarios. We will distinguish between two cases. When $\Delta f_d = 0$, we obtain

$$T_m = A_m \times N$$
$$\times \begin{cases} \cos^2\mu + \sin^2\mu\cdot(1 - 2|\Delta\varphi|/\pi), & \Delta f_0 = 0 \\ \mp\frac{2}{\pi}\sin\mu\cos\mu[e^{\mp j\varphi} - e^{\mp j\varphi'}], & \Delta f_0 = \pm f_d \\ -\frac{2}{\pi}\sin^2\mu e^{\mp j(\varphi+\varphi')}\sin|\Delta\varphi|, & \Delta f_0 = \pm 2f_d \end{cases}. \tag{30}$$

In (30), we are ignoring the terms corresponding to $|\Delta f_0| > 2f_d$ since they will be negligible in the probability calculations. When the actual and assumed tone frequencies are not the same, i.e., $\Delta f_d \neq 0$, and assuming f_d is not a multiple of f_d' and vice versa, we get

$$T_m = A_m \times N$$
$$\times \begin{cases} \cos^2\mu, & \Delta f_0 = 0 \\ \mp\frac{2}{\pi}\sin\mu\cos\mu e^{\mp j\varphi}, & \Delta f_0 = \pm f_d \\ \pm\frac{2}{\pi}\sin\mu\cos\mu e^{\mp j\varphi'}, & \Delta f_0 = \pm f_d' \\ -\frac{4}{\pi^2}\sin^2\mu e^{\mp j(\varphi+\varphi')}, & \Delta f_0 = \pm(f_d + f_d') \\ \frac{4}{\pi^2}\sin^2\mu e^{\mp j\Delta\varphi}, & \Delta f_0 = \pm\Delta f_d \end{cases} \tag{31}$$

where for simplicity we are ignoring terms that include factors c_k for $|k| \geq 3$. If $\Delta f_1 = 0$ and $\Delta f_d = 0$, from (30) and (25), we obtain

$$\begin{cases} \lambda_1, & \text{if } \Delta f_0 = 0 \\ \lambda_2, & \text{if } \Delta f_0 = \pm f_d \\ \lambda_3, & \text{if } \Delta f_0 = \pm 2f_d \\ \lambda_0, & \text{otherwise} \end{cases}$$

and if $\Delta f_1 = 0$ and $\Delta f_d \neq 0$, using (31) and (25), we arrive at

$$\lambda = \begin{cases} \lambda_4, & \text{if } \Delta f_0 = 0 \\ \lambda_5, & \text{if } \Delta f_0 = \pm f_d, \pm f_d' \\ \lambda_6, & \text{if } \Delta f_0 = \pm(f_d + f_d'), \pm\Delta f_d \\ \lambda_0, & \text{otherwise} \end{cases}$$

where the λ_i are given in (25).

REFERENCES

[1] S. G. Udomkesmalee and S. A. Hayati, "Mars science laboratory focused technology program overview," in *Proc. IEEE Aerospace Conf.*, Big Sky, MT, Mar. 2005, pp. 961–970.

[2] A. Steltzner *et al.*, "Mars Science Laboratory entry, descent, and landingsystem," in *Proc. IEEE Aerospace Conf.*, Big Sky, MT, Mar. 2006, pp. 1–15.

[3] R. Mitcheltree, A. Steltzner, A. Chen, M. San Martin, and T. Rivellini, "Mars science laboratory entry, descent and landing system verificationand validation program," in *Proc. IEEE Aerospace Conf.*, Big Sky, MT, Mar. 2006, pp. 1–6.

[4] D. D. Morabito and K. T. Edquist, "Communications blackout predictions for atmospheric entry of mars science laboratory," in *Proc. IEEE Aerospace Conf.*, Big Sky, MT, Mar. 2005, pp. 489–500.

[5] E. Satorius, P. Estabrook, J. Wilson, and D. Fort, Direct-To-Earthcommunications and Signal Processing for Mars Exploration Rover entry, Descent and Landing JPL IPN Progress Rep. 42-153, May 2003.

[6] W. J. Hurd, P. Estabrook, C. S. Racho, and E. H. Satorius, "Criticalspacecraft-to-earth communications for mars exploration rover (MER) entry, descent and landing," in *Proc. IEEE Aerospace Conf.*, 2002, vol. 3, pp. 1283–1292.

[7] D. C. Rife and R. R. Boorstyn, "Single-tone parameter estimation fromdiscrete-time observations," *IEEE Trans. Inform. Theory*, vol. IT-20, no. 5, pp. 591–597, Sep. 1974.

[8] S. Kay, "A fast and accurate single frequency estimator," *IEEE Trans. Acoust., Speech, Signal Process.*, vol. 37, no. 12, pp. 1987–1990, Dec. 1989.

[9] P. M. Djuric and S. M. Kay, "Parameter estimation of chirp signals," *IEEE Trans. Acoust., Speech, Signal Process.*, vol. 38, no. 12, pp. 2118–2126, Dec. 1990.

[10] C. Lin and P. M. Djuric, "Estimation of chirp signals by MCMC," in *Proc. IEEE Conf. Acoustics, Speech and Signal Processing (ICASSP)*, Istambul, Turkey, Jun. 2000, vol. 1, pp. 265–268.

[11] A. S. Kayhan, "Difference equation representation of chirp signalsand instantaneous frequency/amplitude estimation," *IEEE Trans. Signal Process.*, vol. 44, no. 12, pp. 2948–2958, Dec. 1996.

[12] S. Barbarossa and O. Lemoine, "Analysis of nonlinear EM signals bypattern recognition of their time-frequency representation," *IEEE Signal Process. Lett.*, vol. 3, no. 4, pp. 112–115, Apr. 1996.

[13] B. Völcker and B. Ottersen, "Chirp parameter estimation from a samplecovariance matrix," *IEEE Trans. Signal Process.*, vol. 49, no. 3, pp. 603–612, Mar. 2001.

[14] M. Z. Ikram, K. Abed-Meraim, and Y. Hua, "Estimating the parametersof chirp signals: An iterative approach," *IEEE Trans. Signal Process.*, vol. 46, no. 12, pp. 3436–3441, Dec. 1998.

[15] A. Papandreou, G. F. Boudreaux-Bartels, and S. M. Kay, "Detection andestimation of generalized chirps using time-frequency representations," in *Proc. Asilomar Conf. Signals, Systems and Computers*, Pacific Grove, CA, Nov. 1994, vol. 1, pp. 50–54.

[16] L. A. Cirillo, A. M. Zoubir, and M. G. Amin, "Estimation of FM parameters using a time-frequency hough transform," in *Proc. IEEE Conf. Acoustics, Speech and Signal Processing (ICASSP)*, Toulouse, France, 2006, vol. 3, pp. 169–172.

[17] F. Gini, M. Montanari, and L. Verrazzani, "Estimation of chirp radarsignals in compound-gaussian clutter: A cyclostationary approach," *IEEE Trans. Signal Process.*, vol. 48, no. 4, pp. 1029–1039, Apr. 2000.

[18] S. Shamsunder and G. B. Giannakis, "Detection and estimation of chirp signals in non-gaussian noise," in *Proc. Asilomar Conf. Signals, Systems and Computers*, Pacific Grove, CA, Nov. 1993, vol. 2, pp. 1191–1195.

[19] C. G. Lopes, E. Satorius, and A. H. Sayed, "Adaptive carrier tracking fordirect-to-earth mars communications," in *Proc. Asilomar Conf. Signals and Systems*, Pacific Grove, CA, Oct. 2006, pp. 1042–1046.

[20] F. Gustafsson, S. Gunnarsson, and L. Ljung, "Shaping frequency-dependent time resolution when estimating spectral properties withparametric methods," *IEEE Trans. Signal Process.*, vol. 45, no. 4, pp. 1025–1035, Apr. 1997.

[21] V. A. Vilnrotter, S. Hinedi, and R. Kumar, "Frequency estimation techniques for high dynamic trajectories," *IEEE Trans. Aerosp. Electron. Syst.*, vol. 25, no. 4, pp. 559–577, Jul. 1989.

Federico S. Cattivelli (S'03) received the B.S. degree in electronics engineering in 2004 from Universidad ORT, Uruguay. He received the M.S. degree in 2006 from the University of California Los Angeles (UCLA), in where he is currently pursuing the Ph.D. degree in electrical engineering.

In 2005, he joined UCLA, where he is currently a member of the Adaptive Systems Laboratory. His research interests are in signal processing, adaptive filtering, estimation theory, and optimization. His current research activities are focused in the areas of distributed estimation over adaptive networks, Doppler shift frequency estimation for space applications (in collaboration with the NASA Jet Propulsion Laboratory), and state estimation and modeling in biomedical systems (in collaboration with the UCLA School of Medicine).

Mr. Cattivelli was recipient of the UCLA Graduate Division and UCLA Henry Samueli SEAS Fellowships in 2005 and 2006.

Polly Estabrook received the B.S. degree in engineering physics and the B.A. degree in economics from the University of California at Berkeley in 1975 and the M.S. and Ph.D. degrees in electrical engineering from Stanford University, Stanford, CA, in 1981 and 1989, respectively.

She is the Deputy Section Manager of the Communications Architectures and Research Section (3320) at NASA's Jet Propulsion Laboratory. Since March 2008, she has served as the Lead System Engineer in NASA's Space Communication and Navigation Program Office directing a team of 20 system engineers responsible for defining the new communication and tracking capabilities needed by NASA's Constellation Program in support of the Vision for Space Exploration. From 2000 to 2004, she was the Lead Telecom System Engineer for the Mars Exploration Project, responsible for the performance of the Entry Descent and Landing telecommunications system and for the overall design and performance of the Direct to Earth and relay communications systems. Before joining JPL, she was a Technical Consultant for a start-up company for TV direct broadcast systems in the Bay Area and a Fellow of the Organization of American States, working on domestic satellite systems in Lima, Peru. Her area of expertise is telecom system engineering, in particular the development of new telecom architectures and networks for future space exploration missions and the application of new communication technologies to space exploration. She is the author of over 35 external publications and the recipient of the NASA Exceptional Achievement Medal for Mars Exploration Rover Telecom System Engineering.

Edgar H. Satorius (M'80) received the B.Sc. degree in engineering from the University of California Los Angeles and the M.S. and Ph.D. degrees in electrical engineering from the California Institute of Technology, Pasadena.

He is a Principal Member of the Technical Staff, Flight Communications Systems Section of the Jet Propulsion Laboratory, Pasadena. He performs systems analysis in the development of digital signal processing and communications systems with specific applications to blind demodulation, digital direction finding, and digital receivers. He has published over 90 articles and holds two patents in the field of digital signal processing and its applications. In addition, he is an Adjunct Associate Professor at the University of Southern California, where he teaches digital signal processing courses.

Ali H. Sayed (F'01) is a Professor and Chairman of Electrical Engineering at the University of California Los Angeles, where he directs the Adaptive Systems Laboratory (www.ee.ucla.edu/asl).

He has published widely in the areas of adaptive systems, statistical signal processing, estimation theory, adaptive and cognitive networks, and signal processing for communications. He has authored or co-authored several books, including *Adaptive Filters* (New York: Wiley, 2008), *Fundamentals of Adaptive Filtering* (New York: Wiley, 2003), and *Linear Estimation* (Upper Saddle River, NJ: Prentice Hall, 2000).

Dr. Sayed has served on the editorial boards of several journals, including as Editor-in-Chief of the IEEE TRANSACTIONS ON SIGNAL PROCESSING. He sits on the Board of Governors of the IEEE Signal Processing Society. His work has received several recognitions, including the 1996 IEEE Donald G. Fink Award, the 2003 Kuwait Prize, the 2005 Terman Award, the 2002 Best Paper Award, and the 2005 Young Author Best Paper Award from the IEEE Signal Processing Society. He has served as a 2005 Distinguished Lecturer of the SP Society and as General Chairman of ICASSP 2008.